Oct 14th, 12:00 AM

Inelastic Performance and Design of Cfs Walls Braced with Straps Having Reduced Width Fuses

Kostadin Velchev

Nisreen Balh

Nineteenth International Specialty Conference on Cold-Formed Steel Structures
St. Louis, Missouri, U.S.A, October 14 & 15 2008

Inelastic Performance and Design of CFS Walls Braced with Straps having Reduced Width Fuses

K. Velchev[1], G. Comeau[1], N. Balh[1] and C.A. Rogers[2]

Abstract

Provisions that address the seismic design of cold-formed steel frame strap braced walls are not provided in the 2005 National Building Code of Canada (NBCC) or in the Canadian Standards Association (CSA) S136 Standard for the design of cold-formed steel structures. Previous research aimed at developing appropriate seismic design provisions for these walls revealed that premature fracture of screw connected flat strap braces can lead to inadequate ductility. A subsequent research project was undertaken to evaluate the inelastic performance of screw connected single-storey braced wall configurations constructed with flat straps having a reduced width fuse. The intent of using a fuse in the brace was to reduce the extent of inelastic demand at the brace connections while confining plastic deformations to a well defined section of the brace. Test walls were specifically designed and detailed following a capacity approach. The strap braces were expected to undergo gross cross-section yielding with strain hardening along the fuse, while the other elements

[1] Graduate Student, Department of Civil Engineering & Applied Mechanics, McGill University, Montreal QC, Canada.
[2] Associate Professor, Department of Civil Engineering & Applied Mechanics, McGill University, Montreal QC, Canada.

in the seismic force resisting system were selected to be able to carry the probable brace capacity. A summary of the test program is provided in the paper, including failure modes and ductility measures, as well as recommendations on how proper seismic detailing may be achieved. The scope of the research also included the determination of preliminary seismic force modification factors for use with the NBCC based on the measured ductility and overstrength of the test walls.

Introduction

The installation of steel strap diagonal cross bracing in a structure (Fig. 1) is an efficient and economical means to resist wind and seismic forces because the diagonals work in axial tension and therefore require only a minimum amount of material to provide adequate lateral stiffness and strength. Nevertheless, the overall lateral strength, stiffness and ductility of this bracing system depends on all the other elements in the seismic force resisting system (SFRS); i.e. strap connections, gusset plates, chord studs and tracks, as well as the anchorage including holddown and anchor rod. In order to limit inelastic deformations under seismic loading to brace yielding the strap braced walls need to be designed and detailed following a capacity approach (Al-Kharat & Rogers, 2007). In this approach an element of the SFRS is chosen to act as a fuse, while the remaining elements in the lateral load carrying path are designed and detailed for the probable capacity of the fuse element (AISI-S213, 2007). The straps are often assumed to act as a fuse element and thus should be able to reach and maintain their yield strength during the repeated displacement cycles of an earthquake. The use of screws to connect the brace ends may result in fracture of the net cross section and lead to sudden failure with a significant reduction of the ductility of the system if proper detailing and material selection are not followed (Al-Kharat & Rogers, 2008). In situations where contractors may not be able to satisfy the specific detailing and material requirements to ensure ductile braced wall performance a possible solution is to use straps having a reduced width fuse. The fuse size can be selected to reduce the inelastic demand at the brace connections and control the probable force level throughout the SFRS.

Figure 1: Example of a CFS structure with constant width strap braces

somewhat modified from that described in AISI-S213 (2007). The scope of study consisted of the monotonic and reversed cyclic testing of walls, evaluation of the performance and the determination of seismic force modification factors based on the measured ductility and overstrength.

Test Program

Tests of ten strap braced stud wall specimens were carried out at McGill University using the loading frame illustrated in Figure 2. These ten 2440 x 2440 mm walls were divided into three configurations that can generally be referred to as light, medium and heavy CFS construction; that is, the expected factored lateral in-plane resistance in a wind and seismic loading situation was assumed to be 20, 40 and 75 kN, respectively. The dimensions of the fuse for each brace were first selected given these three lateral loads and the assumption that tension straps would be placed on both sides of each wall. The other elements in the seismic force resisting system were then designed following capacity principles; all of the components in the SFRS were expected to be able to carry the force associated with the probable ultimate capacity of the tension braces without exhibiting extensive damage.

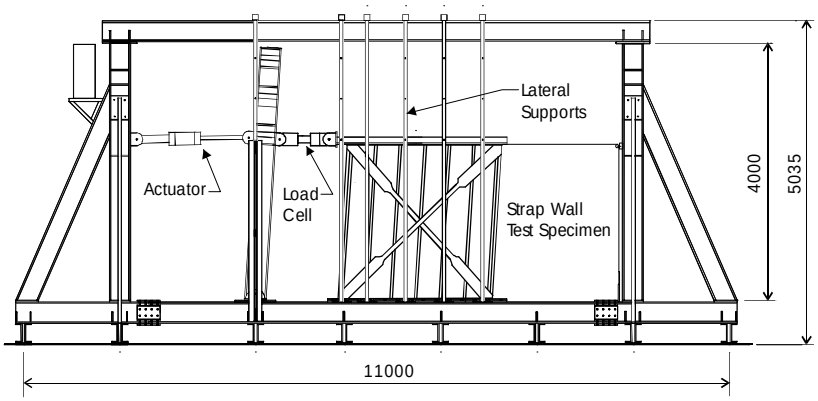

Figure 2: Schematic drawing of displaced 2440 × 2440 mm strap braced wall specimen in test frame

The components of each wall are described in Table 1. All structural members were of ASTM A653 steel (2005). In order to increase the axial capacity of the chord studs such that the vertical component of the brace force could be carried they were composed of two C-sections connected back-to-back using two No. 10 × ¾" wafer head framing screws spaced at 305 mm o/c. The interior studs were placed at a spacing of 406 mm.

Following the details used by Al-Kharat and Rogers (2008) all walls were constructed with an extended track. Connections between the studs and tracks were made with No. 8 × ½" wafer head framing screws, whereas the strap braces were connected to the frame members or gusset using No. 10-3/4" wafer head self drilling screws. The gusset plates, when used, were in turn attached to the framing members using No. 10-3/4" wafer head self drilling screws. Simpson Strong-Tie S/HD10S holddown anchors were installed in all four corners of the light walls, and S/HD15S holddowns were similarly installed in the medium and heavy walls.

Table 1: Matrix of strap braced wall test specimens

Specimen Properties[a]	**Test Specimens**					
	Light		**Medium**		**Heavy**	
Test Protocol	Monotonic	CUREE Reversed Cyclic	Monotonic	CUREE Reversed Cyclic	Monotonic	CUREE Reversed Cyclic
Reduced Braces, Short Fuse	25A-M	26A-C	27A-M	28A-C	29A-M	30A-C
Reduced Braces, Long Fuse	31A-M	32A-C	-	-	33A-M	34A-C
Strap Bracing (X-brace on both sides of wall)						
Thickness, in (mm)	0.043 (1.09)		0.054 (1.37)		0.068 (1.73)	
Fuse Width, in (mm)	2.5 (63.5)		2.75 (69.9)		4 (101.6)	
End Width, in (mm)	3.75 (95.2)		4.25 (108)		6 (152.4)	
Grade, ksi (MPa)	33 (230)		50 (340)		50 (340)	
Chord Studs (Double studs screwed together back-to-back)						
Thickness, in (mm)	0.043 (1.09)		0.054 (1.37)		0.068 (1.73)	
Dimensions, in (mm)	3-5/8x1-5/8-1/2 (92.1x41x12.7)		6x1-5/8x1/2 (152x41x12.7)		6x1-5/8x1/2 (152x41x12.7)	
Grade, ksi (MPa)	33 (230)		50 (340)		50 (340)	
Interior Studs						
Thickness, in (mm)	0.043 (1.09)		0.043 (1.09)		0.043 (1.09)	
Dimensions, in (mm)	3-5/8x1-5/8x1/2 (92.1x41x12.7)		6x1-5/8x1/2 (152x41x12.7)		6x1-5/8x1/2 (152x41x12.7)	
Grade, ksi (MPa)	33 (230)		33 (230)		33 (230)	
Tracks						
Thickness, in (mm)	0.043 (1.09)		0.054 (1.37)		0.068 (1.73)	
Dimensions, in (mm)	3-5/8x1-1/4 (92.1x31.8)		6x1-1/4 (152x31.8)		6x1-1/4 (152x31.8)	
Grade, ksi (MPa)	33 (230)		50 (340)		50 (340)	
Gusset Plates						
Thickness, in (mm)	NA		0.054 (1.37)		0.068 (1.73)	
Dimensions, in (mm)	NA		9x7 (229x179)		10x8.5 (254x216)	
Grade, ksi (MPa)	NA		50 (340)		50 (340)	
Nominal compression, tension and bearing capacity of tracks using CSA S136						
Compression[b] (kN)	23.8		48.1		73.9	
Tension[c] (kN)	38.5		100.5		126.9	
Tension[d] (kN)	44.5		119.5		150.8	
Bearing[e] (kN)	14.5		30.6		116.2	
Bearing[f] (kN)	14.7		33.5		50.0	
Nominal axial compresion capacity of chord studs using CSA S136						
Compression[g] (kN)	66.9		117.6		159.5	
Compression[h] (kN)	58.5		102.5		136.5	
Probable forces in SFRS						
$A_g R_t F_u$ Single Brace (kN)	25.7		47.4		87.0	
Total Horizontal Force[i](kN)	36.3		67.0		123.0	
Total Vertical Force[i] (kN)	36.3		67.0		123.0	

[a]Nominal dimentions and material properties [b]Web holes not considered [c]Gross section yielding, web holes not considered [d]Net section fracture, 22.2 mm hole for shear anchor considered [e]Per shear anchor [f]Per anchor rod [g]Web connections at 305 mm o/c & web holes not considered [h]Web connections at 305 mm o/c & 36 mm web holes considered [i]Total force baced on probable nominal capacity of two tension braces

Wall Design

Once the fuse width and thickness had been selected (Table 1) based on the factored load level the design of other components in the SFRS was carried out following capacity principles. The approach was modified from that currently found for limited ductility walls in AISI-S213 (2007) to account for the possibility of strain hardening in the braces. The probable yield capacity of a tension brace, T_n, is defined in AISI-S213 as shown in eq. 1. However, because the fuse length was significantly shorter than the braces, it was necessary to account for strain hardening given the expected lateral drift of the wall. For this reason the probable ultimate capacity of the braces, T_u, (eq. 2) (Table 1) was used to conservatively calculate the design forces in the other SFRS components, including; the brace connections, chord studs, track, gusset plates, anchor rods, holddowns and shear anchors.

$$T_n = A_g R_y F_y \quad (1)$$

$$T_u = A_g R_t F_u \quad (2)$$

where A_g is the gross cross-sectional area of the fuse, and F_y and F_u are the minimum specified yield and ultimate strengths. The variables R_y and R_t are used with the minimum specified material strengths (R_yF_y and R_tF_u) to obtain the probable material strength. AISI-S213 lists values for R_t of 1.2 & 1.1 and for R_y of 1.5 & 1.1 for the 230 & 340 MPa steels, respectively.

It was also necessary to define the length, l, of the fuse in each brace, which was done using eq. 3.

$$l \geq \Delta \cos\alpha / \varepsilon \quad (3)$$

where Δ is the maximum expected lateral drift of the wall, ε is the minimum expected strain capacity of the material and α is the angle of the brace with respect to horizontal. In a real design situation the maximum drift could be taken as the inelastic storey drift limit as defined in the relevant standard. However, this would likely result in a relatively short fuse and extensive strain hardening in the brace. Two fuse lengths were used for the test walls; the first of which was determined assuming that the maximum displacement was Δ = 120 mm, which corresponds to a storey drift of 5%. The minimum elongation in a 50 mm gauge length as defined in ASTM A653 (2005) for 230 MPa SS steels

could be used for the braces of the light walls (i.e. ε = 20%), and for 340 MPA SS Class 1 could be used for the medium and heavy wall configurations (i.e. ε = 12%). In order to obtain a constant fuse length for all walls a lower bound value of ε = 12% was utilized, which resulted in a fuse length of 707 mm. This value was rounded to 30" (762 mm). Note, the 2440 x 2440 mm walls had a brace angle of 45^o. Also, walls with a 60" (1524 mm) fuse were designed and tested to investigate the influence of fuse length. Schematic drawings of all straps, which were fabricated using a Trumpf 2D flatbed laser cutting machine, are provided in Fig. 3. Note, for each wall configuration two monotonic tests were carried out, one of which had screws attaching the strap to the interior studs. Similarly the interior straps of the cyclic tests were connected to the interior studs to identify the impact of additional screw holes in the brace.

The chord studs were designed assuming a concentrically applied compression (vertical) force (Table 1). The back-to-back C-sections were considered to have unbraced lengths of 2440 mm in the strong axis and 1220 mm in the weak axis due to the installation of bridging at mid-height of the walls. The web knock out holes as well as the fastener screw spacing were considered in the design. Chord stud tests showed that an effective length factor of k = 0.9 is reasonable. Nominal capacities were used (ϕ = 1.0) because design level earthquakes are rare, having a return period of 1 in 2500 years, and due to the use of the probable strap force to obtain the chord stud load. The stud capacities were calculated in accordance with CSA S136 (2004) (Table 1).

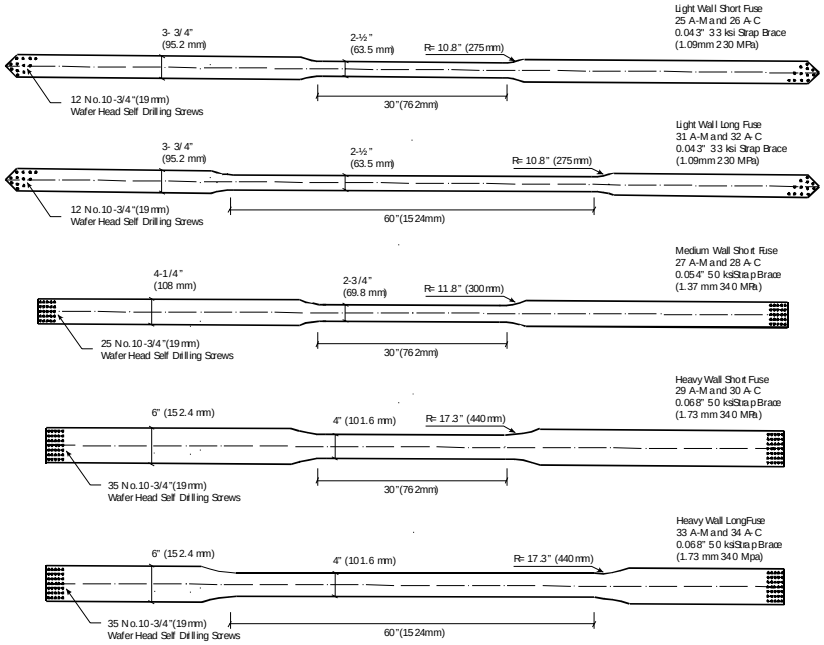

Figure 3: Schematic drawings of straps having reduced width fuse

The horizontal component of the brace force (Table 1) must be transferred through the track element to the supporting structure. The axial capacity of the track in tension, as well as the bearing capacity of the track at the anchor rod and shear anchor locations were determined. Since extended track sections (Figs. 4-5) were used the track was assumed to be placed in tension (Al-Kharat & Rogers, 2008). The horizontal brace force was directed through the extended track by means of the extra shear anchor added outside of the wall footprint. For the heavy walls the bearing capacity of the track alone was not sufficient, therefore a 2.46 mm thick 340 MPa steel plate, 80 x 100 mm, was welded to the track to increase its bearing capacity.

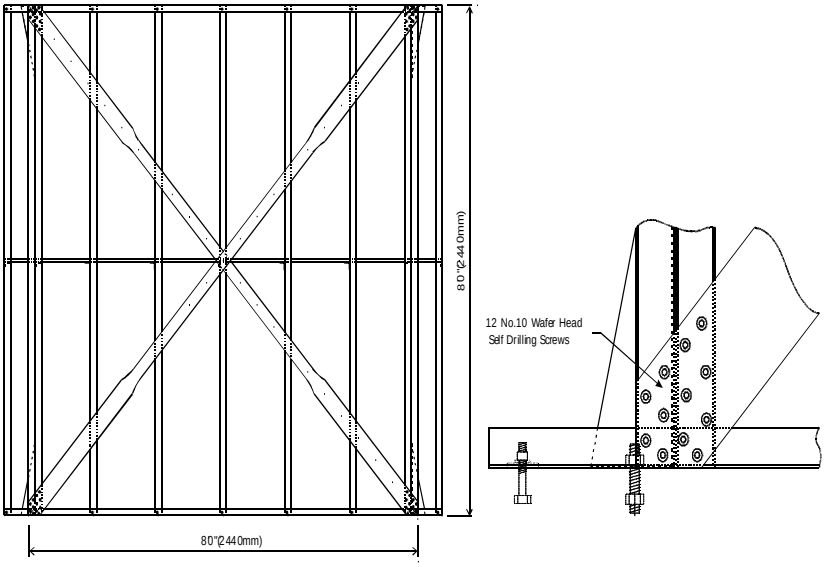

Figure 4: Schematic drawing of light test wall with long fuse

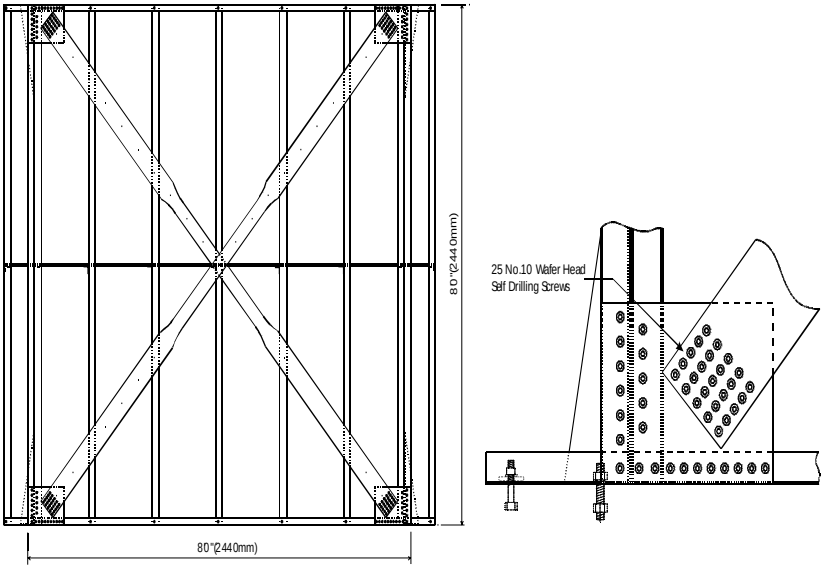

Figure 5: Schematic drawing of medium test wall short fuse

Once the chord stud and track members were selected for each specimen the brace screw connections and gusset plates were designed. The factored shear capacity of the screw connections (CSA S136, 2004) as provided by the manufacturer were compared with the probable capacity of the brace. It was also necessary to ensure that the braces did not fail by fracture at the connection; that is, the net section tension capacity at the connection must exceed the probable ultimate cross-section capacity of the fuse (eq. 4). An increase in the nominal tension resistance (A_nF_u) by the factor R_t = 1.2 (230 MPa material) or 1.1 (340 MPa material) was also considered appropriate since the yield capacity of the material had been increased in the calculation of the probable brace force. The light walls had no gusset plates and the straps were attached directly to the chord stud and track (Fig. 4). In contrast, gusset plates were used in the construction of the medium and heavy walls (Fig. 5). The size and thickness of the gusset plates were chosen considering the Whitmore section subjected to axial tension. The screw connections between the gusset plate, chord stud and track were designed to resist the vertical and horizontal components of the probable strap force.

$$\boldsymbol{A_n R_t F_u \geq A_g R_t F_u} \qquad (4)$$

where A_n is the reduced cross-sectional area of the brace at its end connection, and A_g is the gross cross-sectional area of the brace at the fuse. The width of the connection section of the brace was chosen so that a simple square pattern of screws could be used. Transfer of the uplift forces from the brace through to the supporting test frame was made possible by means of holddown devices from Simpson Strong-Tie and the appropriate size and grade of anchor rods selected from the manufacturer's design catalogue.

Lateral Testing of Wall Specimens

All wall specimens were tested under lateral in-plane loading (Fig. 2) using displacement controlled monotonic and reversed cyclic protocols. Measurements consisted of strap width, in-plane wall displacements, strains in the steel straps, acceleration of the loading beam assembly, and the shear load at the wall top. A steady rate of displacement (2.5 mm/min) starting from the zero load position was applied during the monotonic load procedure. Loading continued until a drop in capacity (below 80% of ultimate) was observed or until the useable travel of the actuator was reached (≈ 200 mm, 8% drift). The Consortium of Universities for Research in Earthquake Engineering (CUREE) ordinary ground motions reversed cyclic load protocol (ASTM E2126, 2005; Krawinkler et al. 2000) was adapted for the cyclic tests. Note, the maximum

displacement cycles for the reversed cyclic tests were approximately ±115 mm (4.5% drift) due to limitations of the actuator's stroke. The yield displacement of the wall, Δ_{sy}, (Fig. 6) was incorporated in the calculation of the reference deformation, Δ. It was assumed that $\Delta = 2.667\ \Delta_{sy}$, where Δ_{sy} was obtained from the nominally identical monotonic wall tests. The complete cyclic loading history for a particular wall configuration was then based upon multiples of the reference deformation. The frequency of the reversed cyclic tests was 0.5 Hz, except toward the end of the protocol where 0.25 Hz was used.

Measured Performance and Modes of Failure

Material tests were carried out for the straps, chords, tracks and gusset plates; the results of the strap tests are reported herein (Table 2). Coupons for each strap size were tested at different speeds, 0.1 mm/min and 100 mm/min. The intent was to represent approximately the brace strain rates of the monotonic (0.000019 s^{-1}) and 0.5 Hz reversed cyclic (0.1 s^{-1}) tests, respectively. Unfortunately the strain rate for the 100 mm/min coupon tests was limited by the capability of the screw driven materials testing machine; nonetheless, the corresponding strain rate was substantially higher than the slowest coupon tests (approximately 1000 times). The measured yield strength, F_y, and tensile strength, F_u, were generally observed to increase for the steels as the strain rate increased; the ratio F_u / F_y exceeded 1.2 as per AISI-S213.

Table 2: Measured material properties of strap braces

Test Specimen	Base Meatal Thickness (mm)	F_y (MPa)	F_u (MPa)	F_u/F_y	% Elong.	F_y/F_{yn}	Test Speed (mm/min)	Strain Rate ($x10^3$ s-1)
25A-M, 26A-C	1.11	296	366	1.24	32.5	1.29	0.1	0.021
31A-M, 32A-C	1.11	314	377	1.20	31.7	1.36	100	20.80
27A-M, 28A-C	1.41	387	560	1.45	27.2	1.14	0.1	0.021
	1.42	406	584	1.44	28.0	1.19	100	20.80
29A-M, 30A-C	1.79	353	505	1.43	32.4	1.04	0.1	0.021
33A-M, 34A-C	1.79	373	521	1.40	31.6	1.10	100	20.80

Note: F_y = measured yield strength, F_u = measured ultimate tensile strength, F_{yn} = minimum specified yield strength

The desirable inelastic behaviour of a cold-formed steel braced wall system is that of gross-cross section yielding of the reduced section of the straps. Ideally, the braces would be able to maintain their yield capacity, and possibly strain harden, over extended lateral displacement of the wall without failure of the other elements in the SFRS; this was the case for most of the specimens that were tested. Figure 7 provides a photograph showing how the inelastic demand was limited to the fuse section of the brace. A second photograph illustrates the different response of two monotonic tests (on the same wall) in which the inner brace was constructed with additional screws. The inner brace fractured at approximately half the storey drift measured for the wall in which the straps

were not screw connected to the interior studs (Fig. 8). The monotonic specimens without additional screws reached a Δ_{max} value exceeding 8% drift. This level of displacement exceeds that which would typically be expected during a design level earthquake. Figures 9 and 10 provide the wall resistance vs. deformation response of representative reversed cyclic tests. None of these specimens exhibited brace fracture even when additional screws were installed; however, drifts of up to approximately 4.5% were applied whereas the monotonic tests were pushed to above 8% drift. Given these observations it is recommended that the reduced fuse section of the brace be treated as a protected zone in which additional screws and holes are not installed; however, the impact of holes on brace ductility diminished as the fuse length was increased. Note, the slight reduction of the wall resistance of test specimen 32A-C (Fig.10) was caused by a block shear failure of the connection between the braces and the flanges of the bottom track, which was not expected, nor observed during the monotonic tests (Velchev, 2008).

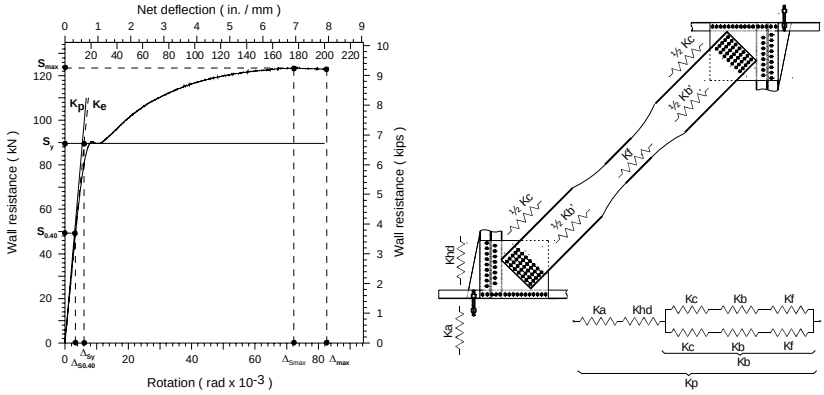

Figure 6: Definition of measured wall parameters and predicted stiffness

Figure 7: Test specimen photographs showing elongated fuse section

The measured yield strength, S_y, of the monotonic tests was obtained using the force level reached soon after yielding commenced (Fig. 6). The maximum lateral force, S_{max}, was higher than S_y because of strain hardening (Table 3). Due to difficulty in identifying the yield level of the cyclic tests S_y was set equal to S_{max}, and thus includes any strain hardening effects (Table 4). The measured elastic shear stiffness, K_e, was defined as the secant stiffness from the zero load level to the 40% of maximum load level, $S_{0.40}$, as recommended in ASTM E2126 (Tables 3-4). The predicted nominal lateral yield strength, S_{yn}, of the wall was based on the tension yield strength of the braces determined using the nominal fuse area (width × thickness) as well as the minimum specified yield strength. S_{yp} is the predicted yield strength of the wall using the measured brace thickness and width of the fuse, as well as the material properties listed in Table 2. The predicted stiffness, K_p, incorporated the stiffness of the brace segments,

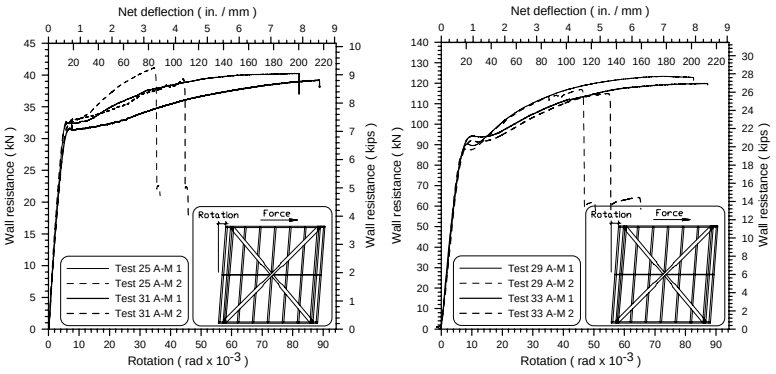

Figure 8: Monotonic resistance light & heavy strap braced walls

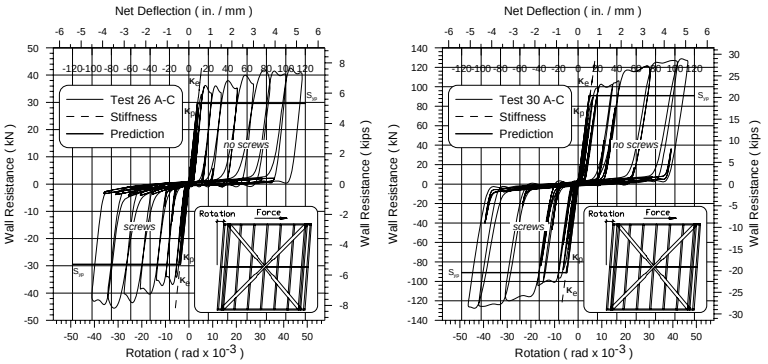

Figure 9: Cyclic resistance light & heavy short fuse strap braced walls

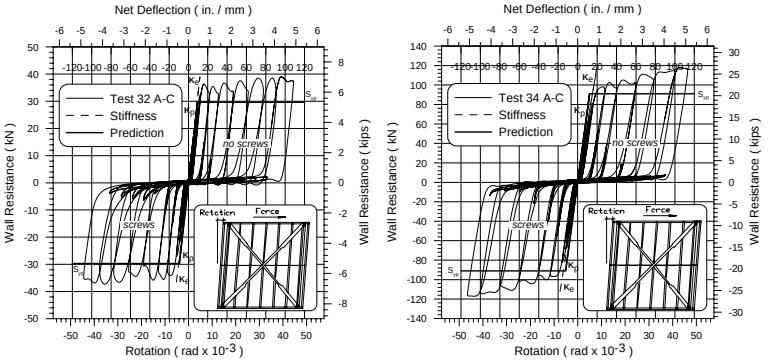

Figure 10: Cyclic resistance light & heavy long fuse strap braced walls

its connections and the holddown and its anchor rod (Fig. 6) using measured properties, whereas K_n incorporated nominal properties. The predicted lateral wall stiffness was reasonable accurate (Tables 3-4) when all of the spring segments shown in Fig. 6 were included. Calculation of K using only the axial stiffness of the braces tends to overestimate the in-plane stiffness of the wall. Predictions

Table 3: Summary of monotonic test information

Test Specimen	K_e (kN/mm)	K_p (kN/mm)	K_n (kN/mm)	K_e/K_p	K_e/K_n	Δ_{max} (mm)	max drift (%)	Energy (Joules)
25A-M 1	2.85	3.34	3.31	0.85	0.86	210	8.62	7294
25A-M 2	3.10	3.34	3.31	0.93	0.94	89	3.66	3006
27A-M 1	4.16	5.20	5.12	0.80	0.81	211	8.64	14333
27A-M 2	4.09	5.20	5.12	0.79	0.80	88	3.59	5126
29A-M 1	6.07	7.79	7.66	0.78	0.79	202	8.27	21796
29A-M 2	6.47	7.79	7.66	0.83	0.84	114	4.66	11595
31A-M 1	2.83	3.15	3.12	0.90	0.91	217	8.88	7496
31A-M 2	2.64	3.16	3.12	0.83	0.85	109	4.48	3695
33A-M 1	6.46	7.40	7.26	0.87	0.89	213	8.73	22474
33A-M 2	5.79	7.40	7.26	0.78	0.80	135	5.54	14524

Test Specimen	S_y (kN)	S_{yp} (kN)	S_{yn} (kN)	S_y/S_{yp}	S_y/S_{yn}	μ (mm/mm)	R_d	R_o
25A-M 1	32.4	29.6	22.5	1.09	1.44	18.5	6.00	1.89
25A-M 2	32.4	29.6	22.5	1.10	1.44	8.5	4.01	2.03
27A-M 1	57.0	53.9	46.0	1.06	1.24	15.4	5.46	1.80
27A-M 2	56.6	53.9	46.0	1.05	1.23	6.3	3.41	1.83
29A-M 1	89.6	91.0	84.5	0.98	1.06	13.7	5.13	1.53
29A-M 2	87.4	91.1	84.5	0.96	1.03	8.4	3.98	1.50
31A-M 1	31.4	29.4	22.5	1.07	1.39	19.5	6.17	1.75
31A-M 2	33.0	29.8	22.5	1.11	1.47	8.7	4.06	1.88
33A-M 1	93.8	91.2	84.5	1.03	1.11	14.7	5.32	1.46
33A-M 2	91.4	91.1	84.5	1.00	1.08	8.6	4.02	1.44

Table 4: Summary of reversed cyclic test information

Test Specimen		K_e (kN/mm)	K_p (kN/mm)	K_n (kN/mm)	K_e/K_p	K_e/K_n	Δ_{max} (mm)	max drift (%)	Energy (Joules)
26A-C	-ve	3.26	3.34	3.31	0.98	0.99	117	4.79	11310
	+ve	3.27	3.34	3.31	0.98	0.99	117	4.79	
28A-C	-ve	4.48	5.20	5.12	0.86	0.88	114	4.66	18837
	+ve	4.45	5.21	5.12	0.85	0.87	114	4.66	
30A-C	-ve	7.34	7.79	7.66	0.94	0.96	113	4.64	29722
	+ve	7.33	7.79	7.66	0.94	0.96	113	4.64	
32A-C	-ve	2.93	3.16	3.12	0.93	0.94	108	4.44	9885
	+ve	3.30	3.16	3.12	1.05	1.06	109	4.45	
34A-C	-ve	6.20	7.40	7.26	0.84	0.85	113	4.64	27519
	+ve	5.96	7.40	7.26	0.81	0.82	113	4.64	

Test Specimen		S_{max} (kN)	S_{yp} (kN)	S_{yn} (kN)	S_{max}/S_{yp}	S_{max}/S_{yn}	μ (mm/mm)	R_d	R_o
26A-C	-ve	45.5	29.5	22.5	1.55	2.02	12.9	4.98	2.24
	+ve	42.5	29.6	22.5	1.43	1.89	12.9	4.98	2.10
28A-C	-ve	77.3	53.9	46.0	1.43	1.68	9.5	4.23	1.87
	+ve	79.6	53.9	46.0	1.48	1.73	9.4	4.21	1.92
30A-C	-ve	127.6	91.0	84.5	1.40	1.51	9.1	4.16	1.68
	+ve	128.9	90.9	84.5	1.42	1.52	9.1	4.15	1.69
32A-C	-ve	37.3	29.7	22.5	1.25	1.66	10.7	4.51	1.84
	+ve	39.0	29.6	22.5	1.31	1.73	12.1	4.81	1.92
34A-C	-ve	117.1	91.1	84.5	1.29	1.39	7.7	3.80	1.54
	+ve	118.0	91.1	84.5	1.30	1.40	7.4	3.72	1.55

for tests run with a monotonic protocol utilized the material properties from coupons tested at 0.1 mm/min, whereas the tests run cyclically at 0.5 Hz were compared with resistances calculated with material properties from coupons tested at 100 mm/min.

Mitchell et al. (2003) describe the basis of the seismic force modification factors listed in the 2005 NBCC (NRCC, 2005). A similar procedure was followed using the data from the strap walls to obtain "test-based" values for R_d and R_o. The ductility related factor, R_d, (eq. 6) was calculated using the ductility, μ, values (eq. 5) listed in Tables 3 and 4.

$$\mu = \frac{\Delta_{max}}{\Delta_{sy}} \tag{5}$$

$$R_d = \sqrt{2\mu - 1} \tag{6}$$

All test specimens showed sufficient ductility such that the calculated R_d values exceed the 2.0 currently found in AISI-S213 for limited ductility strap braced systems. The overstrength related seismic force modification factor, R_o, can be estimated by considering the product of $R_{yield} = S_y / S_{yn}$ and the inverse of the resistance factor, $R_\phi = 1 / \phi = 1 / 0.9 = 1.11$. Note, the test R_{yield} also includes any strain hardening, R_{sh}, exhibited by the braces up to a drift of 4%. Note, the heavy walls 29A-M 1, 29A-M 2, 33A-M 1 and 33A-M 2 provided R_o values that were less than the other tested walls. This can be attributed to the ratio of F_y / F_{yn} of the braces which was only 1.04 (Table 2). Typically, this ratio is 1.1, as defined by R_y for 340 MPa grade steel. The material properties of the heavy braces were near the lower bound of what would normally be obtained from a mill. Furthermore, the R_o calculation approach neglected other factors that would further increase the overstrength; ***i.e.*** member oversize and development of a collapse mechanism. Nonetheless, the calculated R_o values for all tests exceeded 1.3, which is listed in AISI-S213.

Conclusions

A series of screw connected walls braced with straps having reduced width fuses were tested to evaluate their ability to reach and maintain the yield strength (with strain hardening) in the inelastic range of deformation. Capacity principles were implemented in the design of the walls and material properties met the requirements of AISI-S213. The walls were, in general, able to achieve their assumed response. It is recommended, however, to use braces with long fuses to limit the degree of strain hardening and to reduce the possible negative effect of screws being installed along the fuse length. Tests showed that holes should not be placed in the reduced section of the brace when short fuses are used. The seismic force modification factors R_d = 2.0 and R_o = 1.3 currently listed in AISI-S213 for use with the NBCC are appropriate for the walls braced with straps having reduced width fuses.

Acknowledgements

The authors would like to acknowledge the support provided by NSERC, CFI, the Canadian Sheet Steel Building Institute and the American Iron and Steel Institute. Materials for the test specimens were provided by Bailey Metal Products Ltd., Simpson Strong-Tie Co. Inc., ITW Buildex and Grabber Construction Products.

References

AISI: North American standard for cold-formed steel framing – lateral design; AISI-S213 2007, American Iron and Steel Institute, Washington, DC.

Al-Kharat, M., Rogers, C.A.: Inelastic performance of screw-connected cold-formed steel strap braced walls; *Canadian Journal of Civil Engineering*, 35(1): 11-26, 2008.

Al-Kharat, M., Rogers, C.A.: Inelastic performance of cold-formed steel strap braced walls; *Journal of Constructional Steel Research*, 63(4): 460-474, 2007.

ASTM; Standard specification for steel sheet, zinc-coated (galvanized) or zinc-iron alloy-coated (galvannealed) by the hot-dip process; ASTM Standard A653 2005, American Society for Testing and Materials, West Conshohocken, Pa.

ASTM; Standard test methods for cyclic (reversed) load test for shear resistance of framed walls for buildings; ASTM standard E2126 2005, American Society for Testing and Materials, West Conshohocken, Pa.

CSA: North American specification for the design of cold-formed steel structural members; Standard CSA-S136 2004; Canadian Standards Association, Mississauga, Ont.

Krawinkler, H., Parisi, F., Ibarra, L., Ayoub, A., Medina, R..; Development of a testing protocol for woodframe structures. Report W-02 2000, Consortium of Universities for Research in Earthquake Engineering (CUREE), Richmond, CA.

Mitchell, D., Tremblay, R., Karacabeyli, E., Paultre, P., Saatcioglu, M., Anderson, D.L.; Seismic force modification factors for the proposed 2005 edition of the National Building Code of Canada, *Canadian Journal of Civil Engineering*, 30(2): 308 – 327, 2003.

NRCC: National building code of Canada. National Research Council of Canada, 2005; Ottawa, ON.

Velchev, K; Inelastic performance of screw connected CFS strap braced walls, Master's thesis, Department of Civil Engineering and Applied Mechanics, McGill University, Montreal, Canada, 2008.